Applied Microbiology and Biotechnology
https://doi.org/10.1007/s00253-023-12712-z

APPLIED MICROBIAL AND CELL PHYSIOLOGY

Lipopeptides from an isolate of *Bacillus subtilis* complex have inhibitory and antibiofilm effects on *Fusarium solani*

Daniélle Santos-Lima[1] · Cristina de Castro Spadari[1] · Vinícius de Morais Barroso[1] · Juliana C. S. Carvalho[2] · Larissa Costa de Almeida[1] · Felipe Santiago Chambergo Alcalde[3] · Marcelo José Pena Ferreira[2] · Miriam Sannomiya[3] · Kelly Ishida[1,4]

Received: 30 May 2023 / Revised: 10 July 2023 / Accepted: 25 July 2023

Abstract

Bacillus subtilis species complex is known as lipopeptide-producer with biotechnological potential for pharmaceutical developments. This study aimed to identify lipopeptides from a bacterial isolate and evaluate their antifungal effects. Here, we isolated and identified a lipopeptide-producing bacterium as a species of *Bacillus subtilis* complex (strain UL-1). Twenty lipopeptides (six iturins, six fengycins, and eight surfactins) were identified in the crude extract (CE) and fractions (F1, F2, F3, and F4), and the highest content of total lipopeptides was observed in CE and F2. The chemical quantification data corroborate with the hemolytic and antifungal activities that CE and F2 were the most hemolytic and inhibited the fungal growth at lower concentrations against *Fusarium* spp. In addition, they caused morphological changes such as shortening and/or atypical branching of hyphae and induction of chlamydospore-like structure formation, especially in *Fusarium solani*. CE was the most effective in inhibiting the biofilm formation and in disrupting the mature biofilm of *F. solani* reducing the total biomass and the metabolic activity at concentrations ≥ 2 μg/mL. Moreover, CE significantly inhibited the adherence of *F. solani* conidia on contact lenses and nails as well as disrupted the pre-formed biofilms on nails. CE at 100 mg/kg was nontoxic on *Galleria mellonella* larvae, and it reduced the fungal burden in larvae previously infected by *F. solani*. Taken together, the lipopeptides obtained from strain UL-1 demonstrated a potent anti-*Fusarium* effect inducing morphological alterations and antibiofilm activities. Our data open further studies for the biotechnological application of these lipopeptides as potential antifungal agents.

Key points

- *Lipopeptides inhibit Fusarium growth and induce chlamydospore-like structures.*
- *Lipopeptides hamper the adherence of conidia and biofilms of Fusarium solani.*
- *Iturins, fengycins, and surfactins were associated with antifungal effects.*

Keywords *Bacillus subtilis* · *Fusarium* · Lipopeptides · Iturin · Fengycin · Surfactin · Antifungal activity

✉ Miriam Sannomiya
miriamsan@usp.br

✉ Kelly Ishida
ishidakelly@usp.br

[1] Institute of Biomedical Sciences, University of São Paulo, São Paulo, SP, Brazil

[2] Institute of Biosciences, University of São Paulo, São Paulo, SP, Brazil

[3] School of Arts, Sciences and Humanities, University of São Paulo, Arlindo Béttio St. 1000, São Paulo, SP 03828-000, Brazil

[4] Department of Microbiology, Institute of Biomedical Sciences, University of São Paulo, Prof. Lineu Prestes Ave. 1374, São Paulo, SP 05508-000, Brazil

Published online: 10 August 2023

Introduction

Microbial secondary metabolites are known as one of the main sources of new compounds for drug discovery and development (Pan et al. 2019). Among various discovered metabolites, lipopeptides from *Bacillus* are the most widely studied and can be divided into three families according to the chemical structure of the non-ribosomal cyclic peptides such as surfactin, fengycin, and iturin (Zhao et al. 2017).

The interest in lipopeptides for medicine, phytosanitary, bioremediation, and food additives has increased (Mnif and Ghribi 2015). Although they are not yet being used in agriculture and/or in the treatment of human diseases, lipopeptide-producer *Bacillus*, such as *Bacillus thuringiensis*, is already used as a biological control of caterpillars in agriculture (Monnerat et al. 2018). In addition, lipopeptides from *Bacillus* spp. can contribute to plant growth and induce a systemic plant defense response and still have an antagonistic effect on phytopathogens (Ongena and Jacques 2008; Falcäo et al. 2014). The use of these lipopeptides in the clinic is widely considered due to a broad biological effect, e.g., anti-inflammatory, antitumor, antiplatelet, anticoagulant, antiviral, antibacterial (Ben Ayed et al. 2015; Zhao et al. 2017), and even as antifungal activity on pathogenic fungi (Ongena and Jacques 2008; Velho et al. 2011; Mnif and Ghribi 2015; Lei et al. 2019).

Fusarium species are plant pathogenic fungi of agronomic importance, mycotoxin producers, and they are also considered opportunistic human pathogens (Ma et al. 2013). *Fusarium* spp. can cause a broad spectrum of infections, including superficial (such as keratitis and onychomycosis), locally invasive, and disseminated infections, and the most frequent species are *Fusarium solani* and *Fusarium oxysporum* (Nucci and Anaissie 2007). Fusariosis antifungal treatment is limited due to the intrinsic resistance of *Fusarium* to drugs or the reduced activity and side effects of antifungals (Zhao et al. 2021). For superficial infections, the following drugs are usually recommended: natamycin and voriconazole for keratitis, and itraconazole, voriconazole, and terbinafine for onychomycosis (Al-Hatmi et al. 2018). In this regard, the search for new, more efficient, and safer antifungal drugs for fusariosis prevention and treatment becomes necessary.

The current study focused on the identification and characterization by HPLC–ESI–MS/MS of lipopeptides produced by an isolate of *Bacillus subtilis* complex and the quantification of total lipopeptides by HPLC–PDA. Finally, we highlighted the toxicity effects and in vitro and in vivo antifungal potential of lipopeptides, especially on *Fusarium* spp., evaluating their inhibitory effects, morphological alterations, and disruption of biofilm formation steps.

Materials and methods

Microorganisms

The bacterium used here was previously isolated from a culture of *Trichoderma reesei*, as a contaminant that showed antagonistic action on fungal growth, at the Biotechnology Laboratory of School of Arts, Sciences and Humanities (USP, Brazil), and it was registered at the Genetic Heritage Management Council (CGEN/SISGEN, Brazil) under the code A2F350D. After the isolation, the bacterium was phenotypically identified as *Bacillus* sp. and then stored in Luria–Bertani (LB) broth (Kasvi, Italy) with 30% glycerol at − 80 °C.

Candida albicans SC 5314, *Cryptococcus neoformans* ATCC 208821 (or H99), *Aspergillus fumigatus* ATCC 16913, *Fusarium oxysporum* ATCC 48112, and *Fusarium solani* CBS 224.34 were stored in brain hearth infusion (BHI) broth (Becton Dickinson and Company, USA) and 20% glycerol at − 80 °C, recovered, and subcultured in Sabouraud dextrose agar (SDA) or potato dextrose agar (PDA) (both from Kasvi, Italy) for 24–72 h at 35 °C.

Molecular identification of the bacterial isolate

The bacterial species identification was performed by sequencing the 16S ribosomal RNA (rRNA) and *rpoB* (β-subunit of the RNA polymerase) genes, amplified with primers designed in the Primer3Plus program (https://www.bioinformatics.nl/cgi-bin/primer3plus/primer3plus.cgi) using the genome sequences of *Bacillus* spp. and *Bacillus subtilis* species complex strains available in the GenBank database (https://www.ncbi.nlm.nih.gov). The primers used were 16S rRNA forward (AAG CAA CGC GAA GAA CCT TA), 16S rRNA reverse (TGT GGG ATT GGC TTA ACC TC), *rpoB* forward (TTA CGG CTG AAG AAC GCC TT), and *rpoB* reverse (ACA GGT GAC GCG ATG TGA AT).

The DNA extraction was performed using Brazol (chloroform-phenol) (Nova Biotecnologia, Brazil). After, 16S rRNA and *rpoB* region fragments were amplified with 12.5 µL of PCR Master Mix (Promega, San Luis Obispo, CA, USA), 6.5 µL of ultrapure water, 2 µL of DNA (40 ng), and 2 µL (20 pmol) of each primer (Thermo Fischer Scientific, Waltham, MA, USA) to a final volume of 25 µL. The amplification program included an initial denaturation (94 °C for 3 min), followed by 35 cycles of denaturation (94 °C for 1 min), annealing at 60 °C for 1 min, and extension at 72 °C for 1 min. A final extension step at 72 °C for 5 min was developed at the end of the amplification.

The purification of the amplified products was performed with a QIAquick PCR Purification Kit (Qiagen, Hilden, Germany) according to the manufacturer's recommendation.

The purified amplicons were prepared for sequencing in Illumina NextSeq equipment (Illumina, USA).

The sequence data were analyzed with the Sequencher 4.1.4 program (www.genecodes.com) and the alignment in the NCBI database (https://www.ncbi.nlm.nih.gov). The molecular identification of bacterium was performed by the analysis of nucleotide sequence similarity to those published in GenBank. The alignment of 16S rRNA and rpoB region sequences from the bacterium genome was performed with ~ 5000 sequences in the GenBank database using the Basic Local Alignment Search Tool (BLAST). In addition, a phylogenetic analysis was performed by the method based on maximum sequence neighbor-joining genetic distances of 0.5 and by MEGA v.11 program to build a phylogenetic tree with nucleotide sequences aligned and suggested by BLAST of bacterial species that presented sequence identity greater than 90%. Then, cutoff values of above 95% in sequence similarity for the deposited 16S rRNA and rpoB sequences were considered to infer the species of the bacterial isolate studied here. Finally, the nucleotide sequences of bacterial isolate have been deposited in the NCBI GenBank database.

Obtention of crude extract and fractions

The bacterium was recovered on LB agar for 16 h at 30 °C, and isolated colonies were inoculated in LB broth and incubated for 16 h at 30 °C under agitation at 140 rpm. Subsequently, 10 µL of this culture was transferred to 1 L Baraka potato broth (200 g potato and 20 g dextrose to 1 L distilled water), for 6 times, and incubated at 30 °C for 96 h at 140 rpm. The lipopeptides produced by the bacterium were obtained from the culture supernatant by a combination of acid and solvent extraction methods. The culture supernatant was obtained by centrifugation at 8000 rpm at 4 °C for 20 min. Then, the supernatant was acidified to pH 2 with 6 M HCl for precipitation (Jemil et al. 2017). The precipitated was obtained by centrifugation at 3000 rpm, washed 3 times with sterile deionized water, and resuspended in deionized water, and pH was readjusted to 6.5 with 6 M NaOH. Then, the samples were freeze-dried at − 55 °C and under vacuum 0.2 bar (Beta 1–8 LD plus, Martin Christ), and after that, the solid materials were stored at − 20 °C.

About 2.6 g of the sample was solubilized in 13 mL of HPLC-grade methanol. After 15 min of centrifugation at 3000 rpm, the supernatant was filtered on a 0.22-µm nylon membrane for removal of bacterial cells and solid residues. The filtered crude extract (CE) was applied on a Sephadex LH-20 gel filtration column (100 × 5 cm i.d., Pharmacia), and the column was eluted with methanol as a mobile phase at a flow of 3 mL/min, producing 193 fractions of 7 mL each. The thin-layer chromatography (TLC) analyses were performed using a mixture of $CHCl_3$/MeOH/H_2O 65:15:1 (v/v) as mobile phase in Silica gel 60 F254 plates (20 × 20 cm, Sigma-Aldrich). The chromatographic plates were developed by spraying 0.25% ninhydrin solution in ethanol followed by heating to detect peptides and free amino groups.

The fractions with similar chromatographic profiles after TLC analyses were combined into 4 groups of fractions (F1, F2, F3, and F4). Then, the solvent was evaporated in a rotary evaporator, and the crude extract and fractions were freeze-dried and stored at − 20 °C until analysis by high-performance liquid chromatography coupled with electrospray ionization tandem mass spectrometry (HPLC-ESI-MS^n) and biological assays.

Chemical characterization of lipopeptides

A Shimadzu HPLC coupled to an amaZon speed ETD (Bruker Daltonics) mass spectrometer with an ESI detector with an ion trap analyzer and ETD (electron-transfer dissociation) was used for the identification of lipopeptides produced by the bacterium. An aliquot of CE, fractions (F1, F2, F3, and F4), and surfactin (*m/z* 1036.34, ≥ 98.0%, Sigma-Aldrich) was dissolved in methanol to obtain a 1000 µg/mL stock solution. A volume of 10 µL of each solution was injected in the HPLC-ESI-MS^n, using a mobile phase composed of A (1% formic acid in ultrapure water) and B (acetonitrile): A:B (50:50) for 3 min, A:B (0:100) for 18 min, and then 100% B for 5 min at a flow rate of 0.8 mL/min in a linear gradient. Then, the analytes were subjected to a capillary voltage of 3 kV, a cone voltage of 15 V, and a source temperature of 120 °C and the data acquisition in positive mode was performed by MS scanning a second analyzer through the mass-to-charge ratio (*m/z*) range from 100 to 2000 Da and the data analyzed by Bruker Compass DataAnalysis 4.3 (Copyright ©2014; Bruker Daltonik GmbH, USA) (Waters Corporation, Milford, USA). Therefore, HPLC–ESI–MS-MS profiles of the lipopeptides from bacterium were analyzed and compared with data previously published.

Quantification of total lipopeptides

For elaboration of calibration curves, the standard surfactin (*m/z* 1036.34, ≥ 98.0%, Sigma-Aldrich) was solubilized in methanol (2 mg/mL) and filtered in a 0.45-µm syringe filter to obtain 10 solutions of concentrations ranging from 2 to 1600 µg/mL. These samples were analyzed in triplicate by a 1260 HPLC system (Agilent, USA), equipped with a quaternary pump, vacuum solvent degasser unit, column oven, and autosampler, coupled to an Agilent diode array detector (DAD). Chromatography was performed with a reverse-phase column (Zorbax C18 150 × 4.6 mm, 3.5 µm; Agilent, USA), and the column temperature was set at 45 °C. An isocratic method was employed with 20% of 0.1% acetic acid in H_2O and 80% of

acetonitrile for 22 min with a flow rate of 1 mL/min. The injection volume of samples was set at 3 µL, and surfactin peaks were detected at 210 nm. All peaks eluting between 5 and 13 min were assigned as surfactin and integrated for further quantification. The average peak areas vs. the concentration of each analyte were used to construct a surfactin calibration curve, and the equation obtained was as follows: $y = 2513.8x - 728.32$; $R^2 = 0.9929$. The limit of detection (LOD) and the limit of quantification (LOQ) were calculated, respectively, as 0.32 µg/mL and 0.96 µg/mL.

To quantify lipopeptide derivatives from the crude extract and fractions, they were solubilized in methanol (2 mg/mL) and filtered using a 0.45-µm syringe filter. The resulting sample was analyzed in triplicate by HPLC–DAD-UV with the same parameters used to elaborate the calibration curve.

Screening for potential antifungal effect

The antifungal activity of crude extract and fractions was evaluated by the broth microdilution technique (CLSI 2017a, b). They were dissolved in 10% DMSO to obtain a concentration of 4096 µg/mL in RPMI 1640 medium (Sigma-Aldrich) buffered with 0.165 M 3-morpholinopropane-1-sulfonic acid (MOPS; Sigma-Aldrich) (or simply RPMI).

The CE and fractions were serially diluted (1:2) in RPMI into 96-well flat-bottom plates, and 100 µL of fungal suspension was added to the wells, obtaining the final fungal concentration at $0.5–2.5 \times 10^3$ colony-forming unit (CFU)/mL (yeast) or 5×10^4 CFU/mL (conidia) and final concentrations of CE and fractions at 2–1024 µg/mL. The microplates were incubated at 35 °C for 24 h (*C. albicans* and *A. fumigatus*), 48 h (*C. neoformans*), and 72 h (*Fusarium* spp.), to visually determine the minimum inhibitory concentration (MIC) of CE and fractions defined as the lowest concentration that inhibits 50% of fungal growth. Amphotericin B was used as a standard antifungal ranging from 0.03 to 16 µg/mL, and the MIC value was defined as the lowest concentration that inhibits 90% of fungal growth. In addition, minimum effective concentration (MEC) against filamentous fungi was determined as the lowest concentration that results in changes in their morphology observed under an inverted microscope (e.g., shortening and hyphae thickness, branching and septation pattern, and others) (CLSI 2017b).

After that, an aliquot of 10 µL from each well was plated on SDA for yeasts and PDA for filamentous fungi and incubated at 35 °C for 24–72 h to determine the minimum fungicidal concentration (MFC) defined as the lowest concentration capable of killing > 99% of the initial fungal inoculum. The assays were performed in duplicate at least three times, and the final data were expressed as a modal mean.

Morphological analysis

Cells from *Fusarium* spp. untreated and treated with MEC and 4 × MEC of CE and fractions (F2 and F3), for 72 h at 35 °C, were fixed with 4% formaldehyde in PBS for 30 min at room temperature. Then, the cells were washed twice with PBS and labeled with calcofluor white (1 mg/mL) for 5 min at room temperature in a dark chamber. After, the fungal cells were observed by light and fluorescence microscopy, and the images were captured under an $EVOS_{fl}$ microscope (Advanced Microscopy Group, USA).

Antibiofilm activity

The antibiofilm activity of CE, F2, and F3 (2 to 64 µg/mL) was evaluated in two phases of the development of *F. solani* biofilms: on the biofilm formation and the mature biofilms (Van Dijck et al. 2018). The fungus was previously cultivated on PDA for 7 days at 30 °C, and the fungal suspension was adjusted to 1×10^5 conidia/mL in RPMI medium.

To assess the activity against biofilm formation, CE, F2, and F3 were serially diluted (1:2) in RPMI medium into wells from 96-well flat-bottom polystyrene plates and 100 µL of the conidial suspension was added to the wells and incubated for 72 h at 35 °C without shaking. For mature biofilm obtainment, 100 µL of conidial suspension was added into the wells from a 96-well plate and incubated at 35 °C without shaking for 72 h. After, the sessile cells (i.e., adherent biofilm cells) were washed twice with PBS and treated with CE, F2, and F3, and incubated for 72 h at 35 °C without shaking.

After the incubation times, the wells were washed twice with PBS, and the metabolic activity of the sessile cells of the biofilms was determined by the XTT (2,3-bis(2-methoxy-4-nitro-5-sulfophenyl)-2*H*-tetrazolium-5-carboxanilide; Sigma-Aldrich) reduction method and the total biomass of biofilms was determined by the violet crystal stain (Luiz et al. 2015). The assays were performed in triplicate at least three times.

Inhibitory effect on the fungal adhesion in contact lenses

Disposable hydrogel contact lenses were used to assess the adhesion of *F. solani* conidia. A volume of 200 µL of conidial suspension in PBS was aliquoted to the wells of a 24-well plate, and 200 µL of CE in PBS was added to obtain final concentrations of 1×10^3 conidia/mL and 8 µg/mL or 32 µg/mL of CE. Then, the contact lens was added to the wells and the plate was incubated at 4 °C for 24 h. After, the lenses were collected and added to 250 µL of PBS and submitted in an ultrasonic bath at 42 kHz for 2 min and 100 µL was cultured on PDA with chloramphenicol (50 µg/mL)

at 30 °C for 96 h to determine the CFU count. The assay was performed in duplicate at least three times, and the data were compared to the untreated control.

Inhibitory effect on the nail fungal infection

Here, we tested the inhibitory effect of CE (8 µg/mL and 32 µg/mL in PBS) against fungal adhesion and mature biofilm on nail surfaces. In this regard, the human nails (5 mm), without previous use of nail polish, were decontaminated in 10% hypochlorite for 10 min, washed numerous times in sterile distilled water, and dried at room temperature before the experiments.

The nails were distributed into 96-well flat-bottom plates, and 50 µL of *F. solani* conidia (1×10^3 CFU/mL) and 50 µL of CE (8 µg/mL or 32 µg/mL in PBS) were added to the plates incubated at 35 °C for 24 h for adherence inhibition analysis. After, the nails were washed twice in PBS, transferred to a tube containing 100 µL of PBS, and sonicated at 42 kHz in an ultrasonic bath for 2 min; then, serial dilutions (1:10) in PBS were performed and plated on PDA with chloramphenicol (50 µg/mL) for 96 h at 30 °C for CFU count.

The biofilms on nail surfaces were obtained by 100 µL of *F. solani* conidia (1×10^3 CFU/mL) in RPMI medium for 24 h at 35 °C using a 96-well plate. After, the nails were washed twice in PBS, transferred to new wells, and treated with 100 µL of CE (8 or 32 µg/mL) in PBS at 35 °C, and every 24 h for up to 72 h, a fresh PBS-containing CE was changed. After 72 h of incubation, the nails were washed twice in PBS and CFU count was performed as described above.

Both assays were performed in duplicate at least three times, and the data were compared to the untreated control.

Toxicity

Hemolytic activity

A 4% suspension of sheep's red blood cells (v/v, in a sterile 5% PBS-glucose solution) was subjected to different concentrations (16–1024 µg/mL) of CE or fractions for 2 h in a water bath at 37 °C. Negative (untreated) and positive (0.1% Triton X-100) controls were included in the test. After incubation, the samples were centrifuged at 1500 rpm for 5 min and the supernatant was analyzed in a spectrophotometer at 540 nm. The hemolytic activity (HA) was calculated as follows: $HA\ (\%) = 100 - [(CP - AT)/(CP - CN) \times 100]$, where CP is the absorbance of the positive control, AT is the absorbance of the test sample, and CN is the absorbance of the negative control. The hemolytic activity of 50% (HA_{50}) was determined using sigmoidal nonlinear regression (Spadari et al. 2019).

Cytotoxicity assay

The non-tumoral fibroblasts (CCD-18Co) were grown in Eagle's minimum essential medium (EMEM) supplemented with 10% fetal bovine serum and 1% penicillin/streptomycin (all from Thermo Fisher Scientific) at 37 °C and 5% CO_2. A suspension of 6×10^3 cells/well was added on 96-well plates incubated for 24 h, and the cell's monolayer was treated with CE (0.0064 to 100 µg/mL) for 72 h at 37 °C and 5% CO_2. After that, the cell viability was analyzed by the 3-(4,5-dimethylthiazol-2-yl)-2,5-diphenyltetrazolium bromide (MTT; Thermo Fisher Scientific) reduction method (Mosmann 1983).

Toxicity in *Galleria mellonella*

Larvae (2.0–2.5 cm in length and ~ 200 mg of body weight) were treated with 10 µL of CE at 100 mg/kg in PBS by inoculating in the last proleg. The mortality and health status of larvae were observed daily for 5 days to construct the survival and morbidity curves (Loh et al. 2013). PBS groups (without and with DMSO at 2.5% or 5%) were included as controls for vehicle and mechanical injury.

Antifungal efficacy in *Galleria mellonella* larvae

Larvae (2.0–2.5 cm of length and ~ 200 mg of body weight) were infected with 20 µL of standardized inoculum at 1×10^7 conidia/mL of *F. solani* CBS 224.34 in the right proleg. After 2 h, the larvae were treated with CE 100 mg/kg or amphotericin B (AMB) 10 mg/kg in the left proleg. In addition, PBS was injected in two other larval groups: uninfected (PBS group) and infected (untreated group) larvae. Then, the larvae (20 per group) were incubated at 35 °C for 7 days and the daily survival and health status of the larvae were analyzed to construct the survival and morbidity curves, respectively. After 24 h of fungal infection, 4 larvae from each group were randomly selected and macerated in 1 mL of PBS, subsequently diluted in PBS, plated on PDA medium, and incubated for 48 h at 35 °C for CFU count.

Statistical analysis

The statistical analyses were performed using Prism v.8 (GraphPad Software Inc., La Jolla, CA, USA), and p values less than 0.05 were considered significant.

Results

Molecular identification of bacterium

The alignment of the 16S rRNA region sequence from the bacterium genome was performed with ~ 5000 sequences

in the NCBI database. The analyzed sequence was 100% identical to the sequences of *Bacillus subtilis* strains published in GenBank, including phylogenetically close species. Previous studies had showed that the rpoB gene sequence is more discriminative than that of 16S rRNA, and its polymorphism can be used to identify cryptic species (Adékambi et al. 2009). Here, the rpoB sequence of bacterium was 100% identical to the sequence of the following cryptic species of the *Bacillus subtilis* complex: *Bacillus velezensis*, *Bacillus amyloliquefaciens*, and *Bacillus subtilis*. The sequences of 16S rRNA (222 bp) and rpoB (308 bp) regions were deposited in GenBank with the ID MK038722 and ID OP683723, respectively (Fig. S1). Therefore, the lipopeptide-producing bacterium used in this work is a species of the *Bacillus subtilis* complex (strain UL-1).

Chemical characterization, identification, and quantification of lipopeptides

The chromatographic profiles and chemical characterization by HPLC–ESI–MS/MS of 20 lipopeptides from CE and fractions (F1, F2, F3, and F4) produced by the strain UL-1 are depicted in Fig. 1 and Table 1, respectively. The identification of lipopeptides was performed by HPLC-ESI/MS–MS analyses and data previously published. Additionally, the mass spectral data of CE and fractions and that of each identified lipopeptide (1–20) can be appreciated in Table S1 and Figs. S2–S9 (supplementary material).

In the retention times of 12.0–16.0 min, the iturins were detected; from 14.8 to 19.9 min, the fengycins; and from 20 to 29 min, the surfactins (Fig. 1, Table 1). The greatest

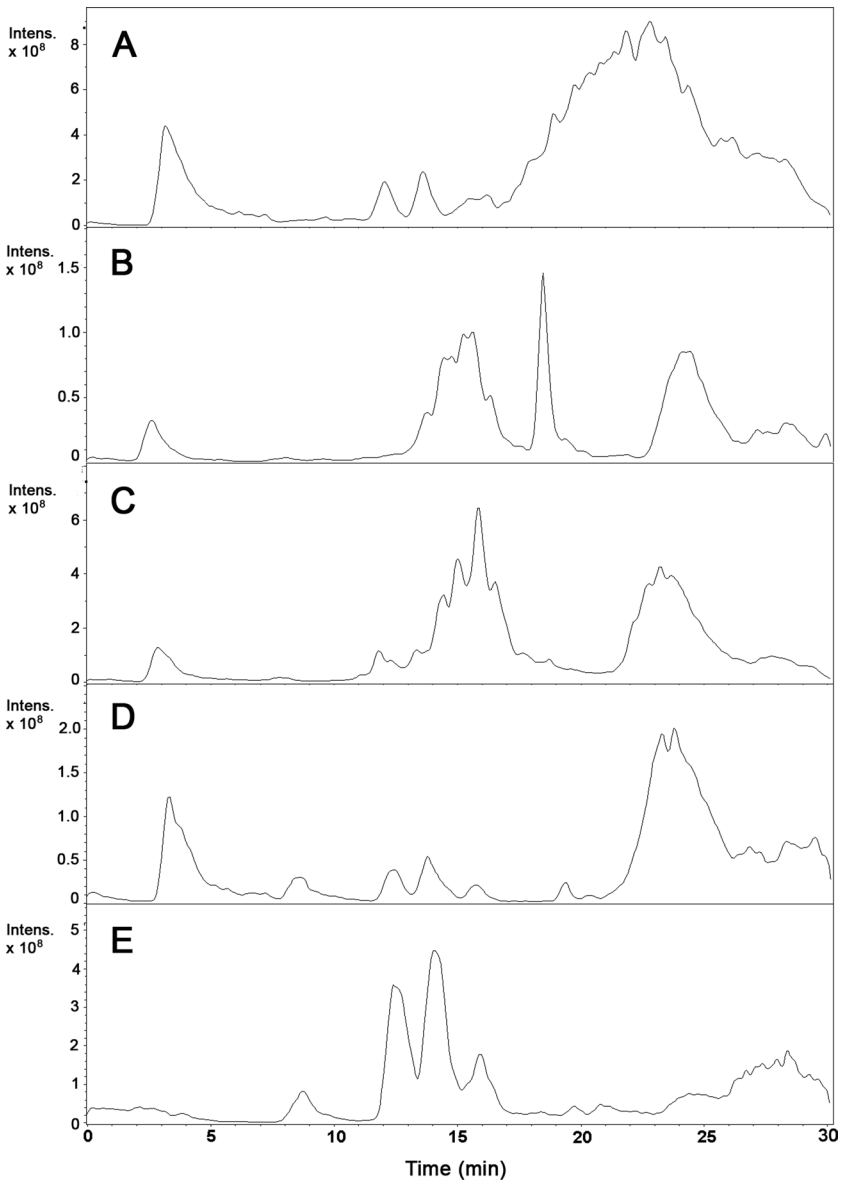

Fig. 1 Chromatograms of crude extract and fractions obtained from the culture supernatant of an isolate of the *Bacillus subtilis* species complex (strain UL-1) obtained by HPLC–ESI–MS/MS. **A** Crude extract. **B** Fraction F1. **C** Fraction F2. **D** Fraction F3. **E** Fraction F4

Table 1 Chemical characterization by HPLC–ESI–MS/MS of lipopeptides from crude extract (CE) and fractions (F1, F2, F3, and F4) produced by an isolate of the *Bacillus subtilis* species complex (strain UL-1)

N°	Lipopeptides	Retention time (min)	*m/z*	Precursor ions	CE	F1	F2	F3	F4
1	Iturin A	12.1	1043.6	C_{14} $[M+H]^+$	x		x	x	x
2	Iturin A	12.3	1065.5	C_{14} $[M+Na]^+$				x	
3	Bacillomycin F	14.1	1057.6	C_{14} $[M+H]^+$	x	x	x	x	x
4	Iturin A	15.8	1071.6	C_{16} $[M+H]^+$	x	x	x	x	x
5	Iturin A	16.9	1079.6	C_{17} $[M+Na]^+$	x			x	
6	Iturin A	27.7	1056.6	C_{15} $[M+H]^+$	x	x	x	x	x
7	Fengycin A	14.8	1463.7	C_{16} $[M+H]^+$	x	x	x		
8	Fengycin B	16.2	1477.7	C_{17} $[M+H]^+$	x	x	x		x
9	Fengycin A	16.3	1435.5	C_{14} $[M+H]^+$	x		x	x	
10	Fengycin B	16.6	1491.7	C_{16} $[M+H]^+$	x	x	x		
11	Fengycin B	16.8	1506.6	C_{18} $[M+H]^+$	x	x	x		
12	Fengycin A	19.9	1451.7	C_{15} $[M+H]^+$	x		x		x
13	Surfactin	21.8	1058.7	C_{16} $[M+Na]^+$	x	x		x	
14	Surfactin	23.5	1036.7	C_{15} $[M+H]^+$	x	x	x	x	x
15	Surfactin	25.2	1022.7	C_{14} $[M+H]^+$	x	x	x	x	x
16	Surfactin	26.8	1044.6	C_{14} $[M+Na]^+$				x	
17	Surfactin	29.0	994.6	C_{12} $[M+H]^+$	x	x	x	x	
18	Surfactin	29.4	1050.6	C_{16} $[M+H]^+$	x		x	x	
19	Surfactin	29.8	1072.7	C_{16} $[M+Na]^+$	x			x	
20	Surfactin	29.9	1008.7	C_{13} $[M+H]^+$	x	x	x	x	

The lowercase letter "x" indicates the detection in the extract and fractions

variety of lipopeptides was identified in CE (five iturins, six fengycins, and seven surfactins). The chromatograms of F1 and F2 were similar, except for the presence of a peak at 18.24 min in F1 (Fig. 1) corresponding to the ion at *m/z* 298, an unidentified non-lipopeptide molecule (Fig. S10, Supplementary material). In F1, three iturin derivatives (3, 4, and 6), four fengycins (7, 8, 10, and 11), and five surfactins (13–15, 17, and 20) were identified (Table 1). In F2, two iturins (1 and 3), five fengycins (7, 8, and 10–12), and four surfactins (14, 15, 17, and 20) were detected. In F3, six iturin derivatives (1–6), one fengycin (9), and seven surfactins (13–18 and 20) were observed, while in F4, only four iturin derivatives (1, 3, 4, and 6), two fengycins (8 and 12), and two surfactins (14 and 15) were detected (Table 1).

According to the quantification assay data in CE and fractions by HPLC–DAD-UV, CE and F2 had a higher content of total lipopeptides than F1, F3, and F4 (Fig. 2, Table S2). In addition, although F2 had a higher content of lipopeptides than CE ($p = 0.0092$, unpaired *t* test), CE contained a greater variety of lipopeptides (18/20) (Table 1).

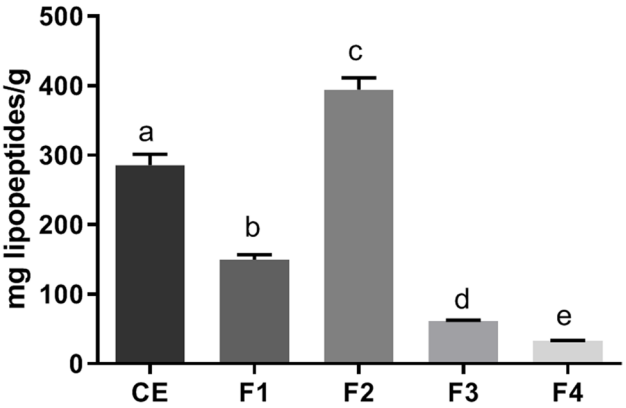

Fig. 2 Quantification of total lipopeptides in the crude extract (CE) and fractions (F1, F2, F3, and F4) obtained from an isolate of the *Bacillus subtilis* complex (strain UL-1) by HPLC–UV-Vis. The letters (a, b, c, d, and e) indicate significant differences between the groups (see statistical analysis in Table S2, unpaired *t* test)

Toxicity

The hemolytic activity was observed for CE and fractions, except for fraction F4. Notably, F3 was less hemolytic compared with CE, F1, and F2 due to a higher concentration for hemolytic activity of 50% (Fig. 3A). Importantly, CE did not show any cytotoxicity on in vitro human fibroblasts even at the highest tested concentration (100 µg/mL, data not shown) and on an in vivo larval model of *G. mellonella* using CE at 100 mg/kg (Fig. 3B, C).

Fungal growth inhibition and morphological alterations of *Fusarium* spp. by secondary metabolites obtained from an isolate of the *Bacillus subtilis* complex

The crude extract and fractions were effective at inhibiting only the growth of *Fusarium* species and *C. neoformans*, but fraction F4 had lower antifungal activity while the standard antifungal AMB inhibited all fungal species tested (Table 2). *Fusarium* spp. were more susceptible to CE due to lower MIC and MEC values. In addition, F2 also showed an effect on fungal morphology at a similar concentration to CE (Table 2).

Morphological analysis using fluorescence microscopy was performed on *Fusarium* cells treated with CE and F2 due to the higher antifungal activity and high lipopeptide content. In addition, we also evaluated the morphological changes caused by F3, as this fraction showed antifungal activity but was less hemolytic. The untreated *Fusarium* spp. had a normal and typical growth of septate and branched hyphae (Figs. 4A, B and 5A, B). The morphological alterations of *Fusarium* spp. were observed after all treatments at MEC values (2–32 µg/mL) and concentrations above such as shortening and/or atypical branching and/or swelling of hyphae forming chlamydospore-like structures (Figs. 4C–H and 5C–H). Interestingly, the inhibition of conidial germination was also observed at concentrations greater than 4 × CEM of CE, F2, and F3 (data not shown). It should be pointed out that these alterations were most prominent in *F. solani* due to a large amount of chlamydospore-like structures after treatments with CE and F2 (apical and intercalary), which was little observed

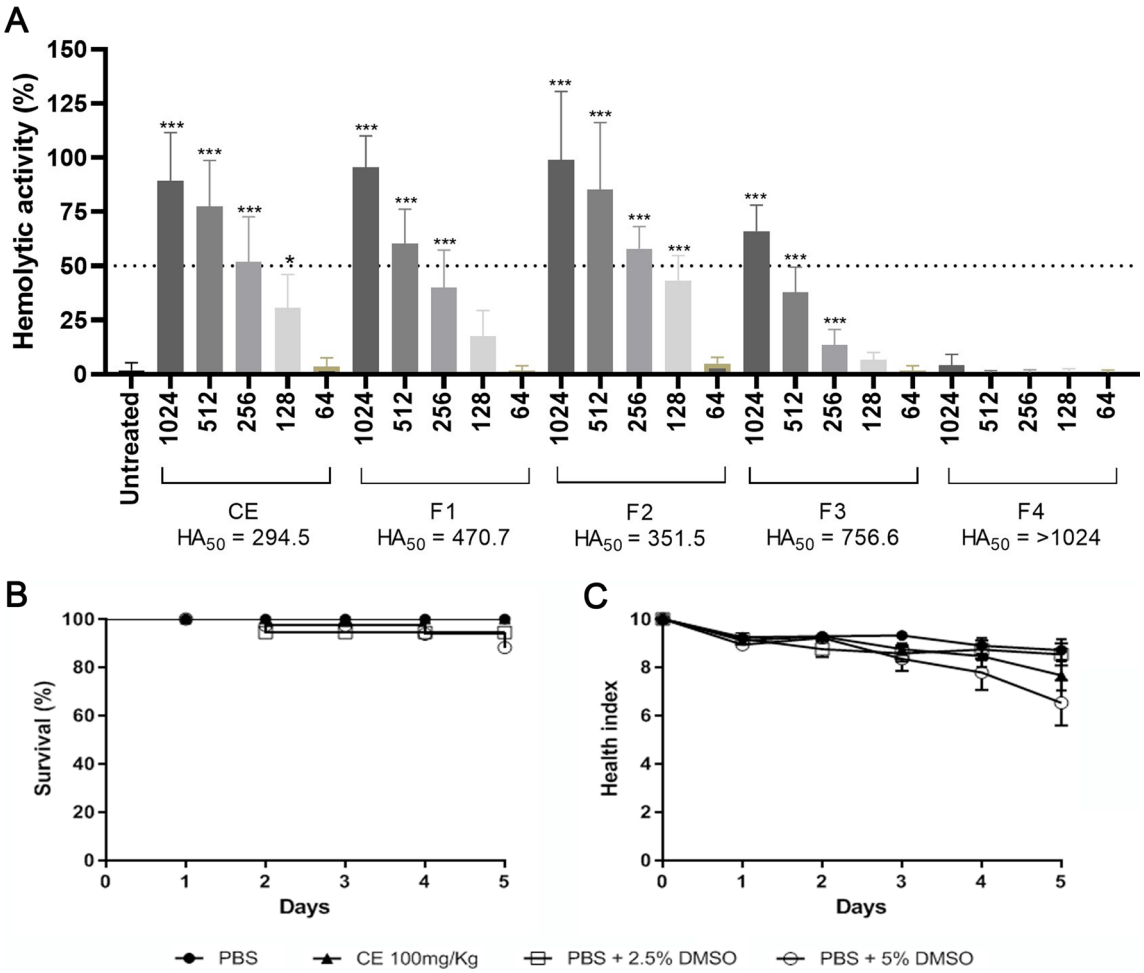

Fig. 3 Hemolytic activity (HA) and toxicity on *Galleria mellonella* larvae of the crude extract (CE) and/or fractions (F1, F2, F3, and F4) obtained from an isolate of the *Bacillus subtilis* complex (strain UL-1). **A** Hemolytic activity of concentrations ranging from 64 to 1024 µg/mL. HA_{50} values, in µg/mL, were obtained by linear regression and indicate the hemolytic activity in 50% of red blood cells compared with untreated cells. Asterisks represent a significant *p* value compared with the untreated group by the one-way ANOVA with Dunnett's post test (*$p < 0.05$ and ***$p < 0.001$). **B** Survival curve and **C** morbidity curve of *Galleria mellonella* larvae untreated (PBS group) and treated with CE (100 mg/kg) and vehicle controls (PBS + DMSO)

Table 2 Antifungal activity of amphotericin B (AMB), crude extract (CE), and fractions (F1, F2, F3, and F4) obtained from a strain of the *Bacillus subtilis* complex against yeasts and filamentous fungi

	Candida albicans	*Cryptococcus neoformans*	*Aspergillus fumigatus*	*Fusarium oxysporum*	*Fusarium solani*
AMB					
MIC	0.12	0.06	0.25	1	2
MEC	nd	nd	0.25	1	2
MFC	0.12	0.06	0.5	2	4
CE					
MIC	> 1024	256	> 1024	32	1024
MEC	nd	nd	> 1024	8	4
MFC	> 1024	> 1024	> 1024	> 1024	> 1024
F1					
MIC	> 1024	256	> 1024	256	1024
MEC	nd	nd	> 1024	16	4
MFC	> 1024	> 1024	> 1024	> 1024	> 1024
F2					
MIC	> 1024	256	> 1024	512	1024
MEC	nd	nd	> 1024	4	2
MFC	> 1024	> 1024	> 1024	> 1024	> 1024
F3					
MIC	> 1024	256	> 1024	64	512
MEC	nd	nd	> 1024	32	32
MFC	> 1024	> 1024	> 1024	> 1024	> 1024
F4					
MIC	> 1024	256	> 1024	512	> 1024
MEC	nd	nd	> 1024	256	> 1024
MFC	> 1024	> 1024	> 1024	> 1024	> 1024

The data are expressed in μg/mL. MIC refers to the lowest concentration that inhibits 50% of fungal growth, MEC refers to the lowest concentration that results in morphological alterations of hyphae (hyphae thickness, branching and septation pattern, and others), and MFC refers to the lowest concentration capable of killing > 99% of the fungal cells

nd not determined

in *F. oxysporum* (Figs. 4 and 5). On the other hand, the standard antifungal AMB showed MEC values equal to MIC values and a similar pattern of morphological alterations emphasizing shorter hyphae and conidial germination inhibition (Table 2; Figs. 4I, J and 5I, J).

Antibiofilm activity

The total biomass and metabolic activity of *F. solani* biofilms were determined after treatment with CE and fractions (F2 and F3) that showed the best antifungal activity on fungal growth and morphology. Here, we tested the antibiofilm effects on two phases of biofilm development: formation and mature biofilms.

CE was the most effective in inhibiting biofilm formation and in disrupting the mature biofilm (Fig. 6). Concentrations ≥ 2 μg/mL and ≥ 4 μg/mL of CE significantly reduced 50–100% the metabolic activity and total biomass, respectively, during biofilm formation ($p < 0.001$, Fig. 6A, D). In addition, CE was able to inhibit the metabolic activity of mature biofilms at ≥ 16 μg/mL (~ 30% of inhibition, $p < 0.001$) but it did not reduce the total biomass (Fig. 6G, J). On the other hand, although fractions F2 and F3 significantly inhibited the metabolic activity and biomass of biofilms, in formation, at concentrations ≥ 2 μg/mL and ≥ 16 μg/mL, respectively (> 40% of inhibition, $p < 0.05$) (Fig. 6B, C, E, F), no antibiofilm effect was observed on mature biofilm (Fig. 6H, I, K, L).

Antifungal effect of crude extract against *Fusarium solani* on the contact lenses and nails

Concentrations at 2 × MEC and 8 × MEC of CE were selected for evaluation of its inhibitory effect on adherence and biofilms of *F. solani* using surfaces of contact lenses and nails due to better antibiofilm activity as mentioned in the section "Antibiofilm activity."

A significant adherence inhibition of 40–60% of *F. solani* conidia was observed after a 24-h treatment with CE at 8 μg/mL and 32 μg/mL on contact lenses and nails,

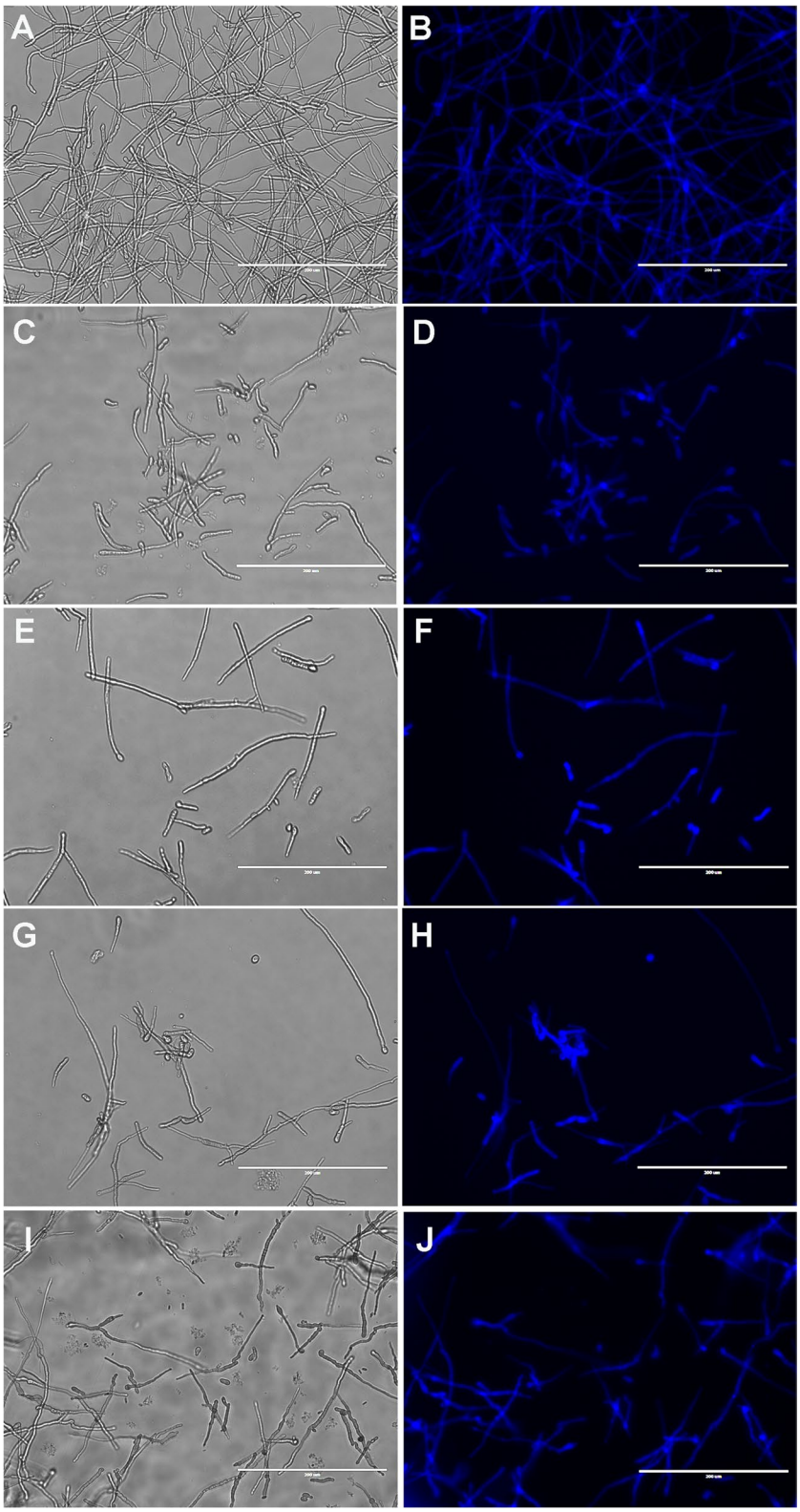

Fig. 4 Images from light (left) and fluorescence (right) microscopy of *Fusarium oxysporum* untreated and treated with 4 × MEC of crude extract, fractions (F2 and F3), and amphotericin B for 72 h at 35 °C. **A**, **B** Untreated. **C**, **D** Crude extract. **E**, **F** Fraction F2. **G**, **H** Fraction F3. **I**, **J** Amphotericin B. Bars = 200 µm

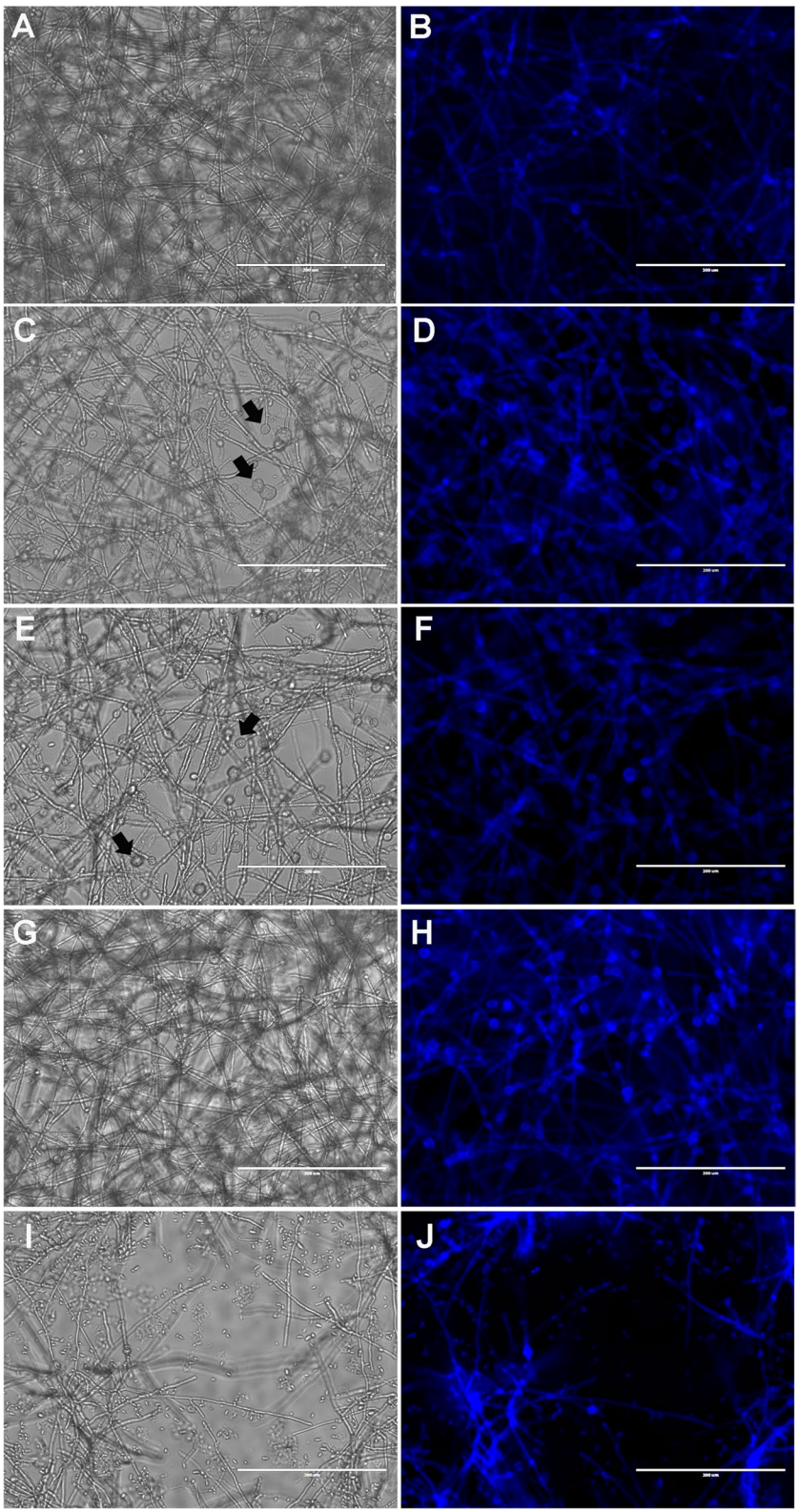

Fig. 5 Images from light (left) and fluorescence (right) microscopy of *Fusarium solani* untreated and treated with 4 × MEC of crude extract, fractions (F2 and F3), and amphotericin B for 72 h at 35 °C. **A**, **B** Untreated. **C**, **D** Crude extract. **E**, **F** Fraction F2. **G**, **H** Fraction F3. **I**, **J** Amphotericin B. Bars = 200 µm. Black arrows indicate chlamydospore-like structures

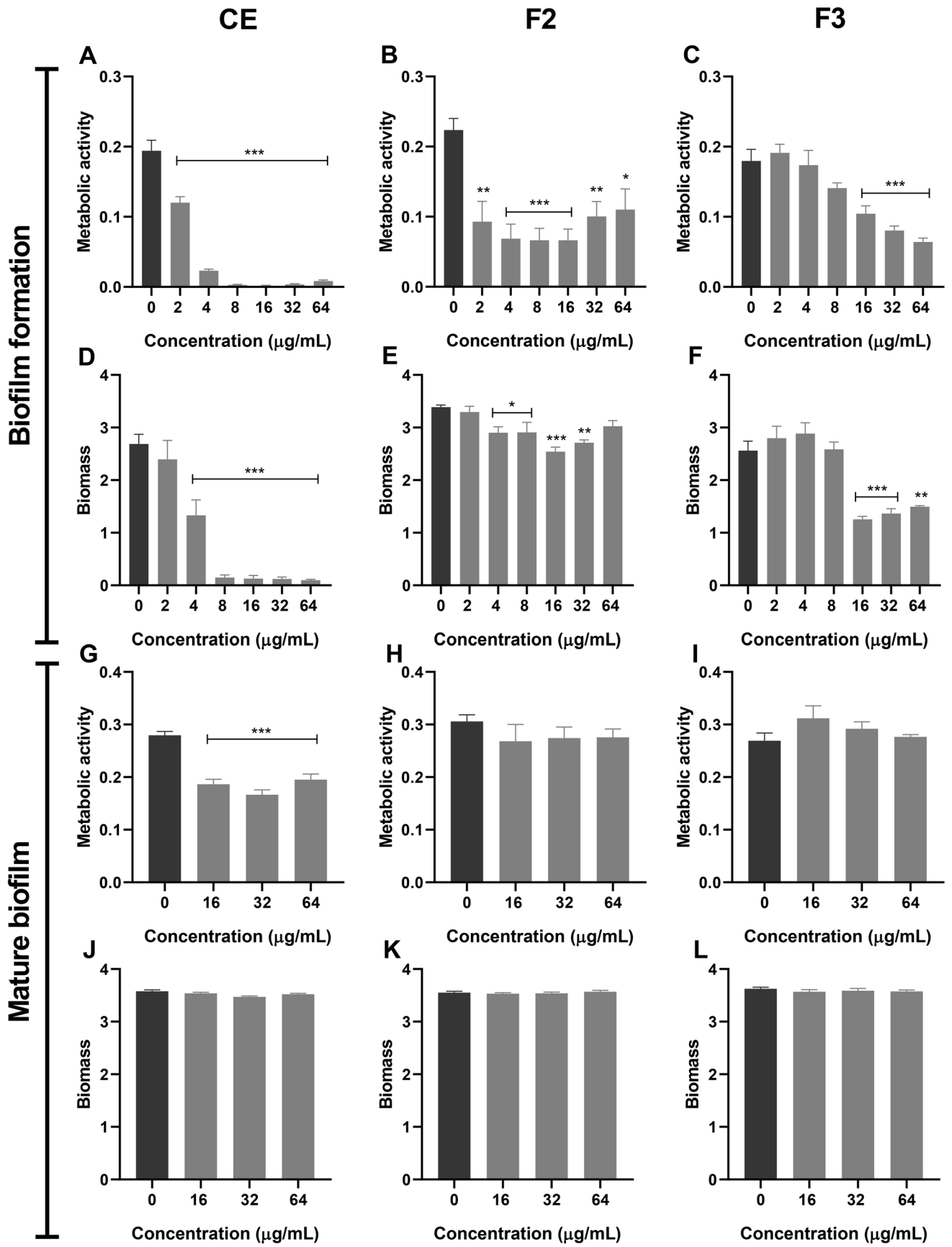
CE
F2
F3
Biofilm formation
Mature biofilm
A
B
C
D
E
F
G
H
I
J
K
L
Metabolic activity
Biomass
Concentration (μg/mL)
0 2 4 8 16 32 64
0 16 32 64
***
**
*

◂**Fig. 6** Antibiofilm activity of crude extract (CE, left column) and fractions F2 and F3 (middle and right columns, respectively) on biofilm formation and mature biofilm of *Fusarium solani*. The metabolic activity of biofilms was determined by the XTT reduction method (**A–C** and **G–I**), and the total biomass was quantified by the crystal violet stain (**D–F** and **J–L**). Asterisks represent a significant *p* value compared with the untreated group (0 group) by the one-way ANOVA with Dunnett's post test (*$p < 0.05$, **$p < 0.01$, and ***$p < 0.001$)

but the inhibition was not different between the two tested concentrations (Fig. 7A, B). On the other hand, although CE at 8 µg/mL had reduced the CFU number, only 32 µg/mL was able to significantly reduce the fungal viability of *F. solani* biofilms on the nails (reduction of ~ 50%, Fig. 7C).

In vivo evaluation of the antifungal activity of the crude extract against *Fusarium solani* infection using a larval model of *Galleria mellonella*

No statistical difference was observed in the survival and morbidity curves between untreated and treated larvae with CE 100 mg/kg and not even for AMB treatment ($p > 0.05$, Fig. 8A, B). Nonetheless, there was a reduction in CFU count in the tissue of larvae treated with CE and AMB, but it was not statistically significant ($p > 0.05$, Fig. 8C).

Discussion

Bacillus species are producers of various secondary metabolites with about 20 classes of compounds (Stein 2005; Sumi et al. 2015; Steinke et al. 2021). They usually produce antifungal metabolites as the non-ribosomal cyclic lipopeptides (surfactins, iturins, and fengycins) and their biosynthesis are regulated by several genes whose transcriptional mechanisms are dependent on environmental conditions (Steinke et al. 2021). Herein, we identified a lipopeptide-producing bacterium by analyzing the 16S rRNA and the rpoB regions as a species of the *Bacillus subtilis* complex, characterized the chemical identity of lipopeptides, and evaluated their antifungal potential.

The most widely used technique for the identification and characterization of lipopeptides is HPLC–ESI–MS/MS (Papayannopoulos 1995; Kato et al. 2011), and we used it to investigate the chemical nature of these compounds in CE and fractions. The molecules were separated and characterized by mass spectral analyses, in positive mode. Then, we identified 20 cyclic lipopeptides from the families of fengycins, iturins, and surfactins. According to the literature, most of these compounds present a fatty acid chain linked to a cyclic peptide structure, which confers greater molecule conformational stability and is associated with biological interactions (Maksimov et al. 2020).

The surfactin family has 20 different structures characterized (Bonmatin et al. 2003). It is an amphiphilic molecule, and its structure typically features a β-hydroxy fatty acid chain linked to a heptapeptide sequence LLDLLDL with Leu and Asp at positions 3 and 6, respectively. At positions 2, 4, and 7, the amino acids reside in Val, Leu, and Ile (Hue et al. 2001; Jacques 2011). Surfactin isoforms occur due to variations in the amino acids of the peptide ring, and MS/MS studies should be performed to identify the sequence establishment for the peptide portion (Yang et al. 2015). According to the HPLC–MS/MS results, the precursor ion at *m/z* 994.6, 1008.7, 1022.7, 1036.7, and 1050.6 was found to be a series of homologous surfactin molecules with a 14-Da difference between their fatty acid chains in their molecular ion species (Table 1, Table S1, and Fig. S9). In addition, $[M + Na]^+$ ions at *m/z* 1044.6, 1058.7, and 1072.7 were also identified as compounds of the surfactin family (Table 1). The fragments at *m/z* 441, 481, 554, 594, 685, 671, 681, and 707 observed in the mass spectra are characteristic marker ions for the identification of the surfactin isoforms (Table 1, Table S1, and Fig. S9).

We identified six fengycins from the CE and fractions. Fengycins are characterized by the presence of a peptide ring containing 8 amino acids (Tyr, Thr, Glu, Ala, Pro, Gln, Tyr, and Ile) and two special amino acids (Orn and Tyr) that bind the peptide ring and the β-saturated or unsaturated fatty acid chain of 14–18 carbon atoms (Cochrane and Vederas 2016). In addition, the presence of fragments at *m/z* 1080 and 966 or at *m/z* 1066 and 952 in the mass spectra indicated the fengycin A isoforms, while the identity ions at *m/z* 1108 and 994 or at *m/z* 1094 and 980 were characterized as a fengycin B isomer (Pueyo et al. 2009).

The fengycins were also detected in this study through the precursor $[M + 2H]^{2+}$ ions at *m/z* 718, 725, 732, 739, 746, and 753 corresponding, respectively, to fengycins at *m/z* 1435.7, 1451.7, 1463.7, 1477.7, 1491.7, and 1506.6 (Table 1, Table S1, and Fig. S8). The presence of the identity ions in the spectra aids in distinguishing the fengycin A and B isomers described previously by Pueyo et al. (2009), and the main difference between the isomers occurs by the presence of an alanine (fengycin A) or valine (fengycin B) at position 6 of the ring (Ma et al. 2016).

The ions at *m/z* 1043.6, 1056.6, 1057.6, 1065.6, 1071.6, and 1079.6 indicated the Asx-Tyr-Asx characteristic fragments of iturin family molecules (Zhao et al. 2018). All these ions, except those at *m/z* 1057.6, were characterized as a homologous series of iturin A, with a difference of 14 Da between the fatty acid chains and the peptide ring containing the amino acid serine in the last

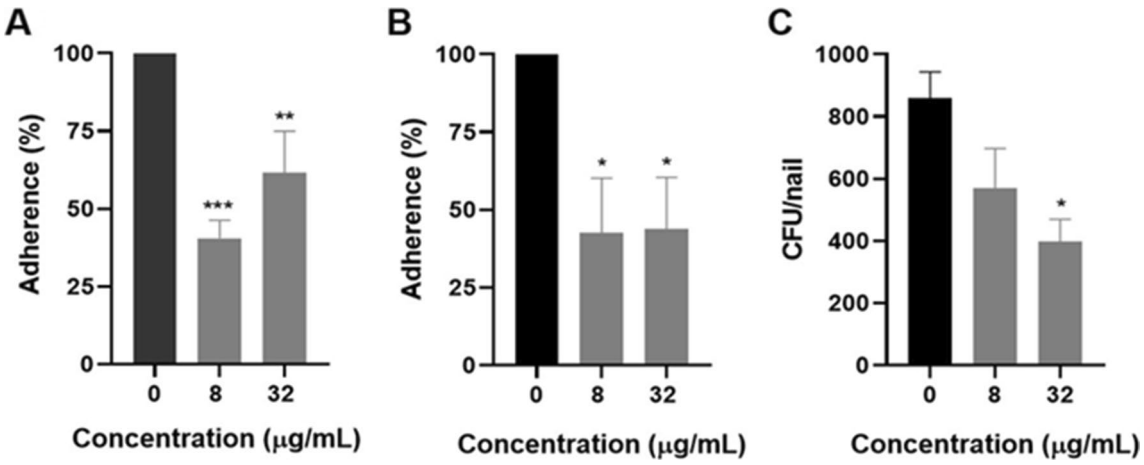

Fig. 7 Antifungal effect of crude extract obtained from an isolate of the *Bacillus subtilis* complex (strain UL-1) against *Fusarium solani* using infection models in contact lenses and nails. **A** Adherence percentage of conidia on contact lenses. **B** Adherence percentage of conidia on nails. **C** CFU count after daily treatment for up to 72 h of the biofilms on nails. Asterisks represent a significant *p* value compared with the untreated group (0 group) by the one-way ANOVA with Dunnett's post test (*$p < 0.05$, **$p < 0.01$, and ***$p < 0.001$)

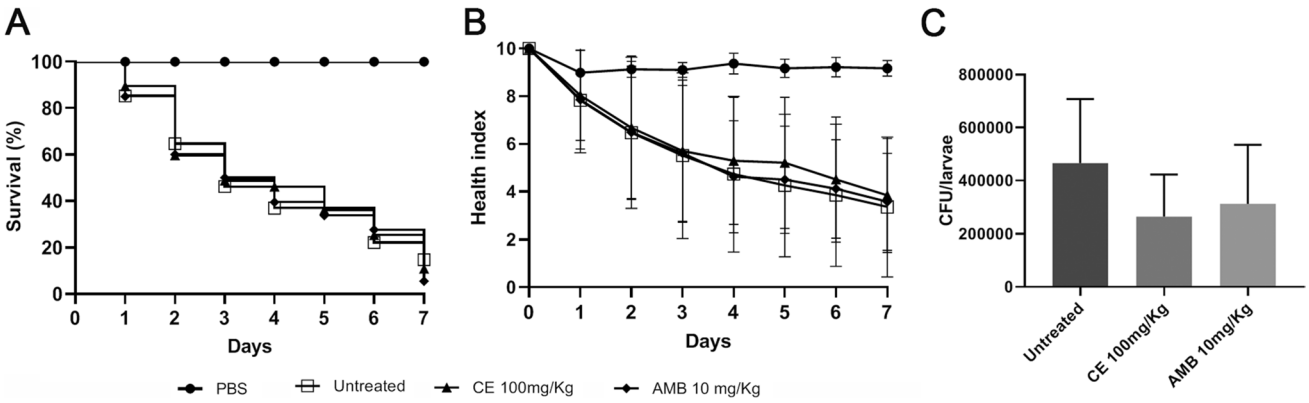

Fig. 8 Antifungal activity of crude extract (CE) obtained from the culture supernatant of an isolate of the *Bacillus subtilis* species complex against *Fusarium solani* infection using a larval model of *Galleria mellonella*. **A** Survival curve, **B** morbidity curve, and **C** fungal burden in the larval tissues. Amphotericin B (AMB) at 100 mg/kg was used as a standard antifungal

position (position 7) linked to the fatty acid chain. While the ion at *m/z* 1057.6 indicates a linear-chain bacillomycin F which contains at position 7 the presence of the amino acid threonine linked to the fatty acid chain (Table 1, Table S1, and Fig. S9).

The biological effects were dependent on lipopeptide concentrations. CE and all fractions contained lipopeptides; however, CE and fraction F2 showed the highest amount of total lipopeptides and greater hemolytic and antifungal activity. Surfactins and iturins are known to have a hemolytic effect and, together, can contribute to a significant increase in hemolysis (Aranda et al. 2005; Ongena and Jacques 2008), while fengycins have low hemolytic activity (Hofemeister et al. 2004). The low hemolytic activity of F3 and F4 can be explained by the low diversity and concentration of lipopeptides.

CE and fractions (F1, F2, and F3) showed fungistatic activity mainly against *C. neoformans* and *Fusarium* spp. However, *F. solani* strain was the most susceptible to the action of lipopeptides obtained from an isolate of the *B. subtilis* complex. The susceptibility of *Fusarium* species to lipopeptides is discussed in the literature regarding growth inhibition and hyphae morphological alterations (Gong et al. 2015; Gu et al. 2017; Cao et al. 2018; Mihalache et al. 2018). In addition, other studies showed an antifungal action of the lipopeptides against other species of phytopathogenic fungi (Kim et al. 2010; Velho et al. 2011; Zhao et al. 2017; Park et al. 2022).

It is important to highlight that CE and fractions F2 and F3 showed lower MIC and MEC values, leading to morphological changes, such as shortening and/or atypical branching and mainly the induction of chlamydospore-like

formation. The same structures were observed in *F. solani* hyphae after treatment with extract from the culture filtrate of *B. subtilis*, and the chlamydospore induction was attributed to the presence of fengycin A homologues (Li et al. 2012). Chlamydospores are fungal resistance structures that act as a survival strategy during undesirable conditions (Hou et al. 2020). Previous studies had demonstrated that calcineurin regulates conidiation, chlamydospore formation, and virulence of *Fusarium* spp., and calcineurin pathway is activated in stress response for the adaptation of fungi (Hou et al. 2020).

The standard antifungal echinocandins, semi-synthetic cyclic lipopeptides, are β-1,3-glucan synthase inhibitors that disrupt the cell wall of *Aspergillus* and *Candida*, affecting the fungal morphology (Kurtz et al. 1994; Nishiyama et al. 2002). Interestingly, echinocandins can induce chlamydospore-like formation, and this cell event is associated to HOG1 pathway activation (Kurtz et al. 1994; Nishiyama et al. 2002; Alonso-Monge et al. 2003). Similarly, fengycin A induces stress response and actives the HOG1 pathway in *C. albicans* (Liu et al. 2019).

The effect of surfactins, iturins, and fengycins on the cytoplasmic membrane causes cell lysis, leading to the leakage of cytoplasmic contents (Seydlová and Svobodová 2008). Therefore, these membrane interactions may have contributed to the hemolytic activity and antifungal effects in *Fusarium* observed here as well as in *Fusarium graminearum*, *F. oxysporum*, and *Colletotrichum acutatum* previously reported (Gu et al. 2017; Mihalache et al. 2018; Park et al. 2022). In addition, other known lipopeptide antibiotics such as polymyxin and daptomycin also interact with bacterial membrane components affecting its permeabilization (Bush 2012).

Biofilms are defined as a multicellular community adhered to a surface and are integrated into an extracellular polymeric matrix. The microbial biofilms are associated with higher tolerance to bioactive molecules (e.g., antimicrobials), environmental stress, and components from the host immune system (Lohse et al. 2018), and these features are the most challenging in eradicating an infection associated with biofilm. Although lipopeptides have been studied against yeast biofilms, e.g., *Trichosporon* spp., *Candida albicans*, and *Mallassezia furfur*, few studies have been carried out on filamentous fungi (Ceresa et al. 2021; Da Silva et al. 2021). In this regard, the lipopeptides studied here in addition to inhibiting the growth of *Fusarium* planktonic cells inhibited the biofilm formation and/or disrupted the mature biofilms of *F. solani* at lower concentrations of CE and fractions F2 and F3. On the other hand, the best one was CE which showed antibiofilm efficacy on both development phases (during biofilm formation and mature biofilm), significantly reducing the total biomass and metabolic activity of sessile cells. Due to better antibiofilm activity and morphological alterations, we choose CE to evaluate its effect in other in vitro models. Then, *F. solani* conidial adhesion on lenses and nails was reduced after treatment with CE for 24 h and the pre-formed biofilms on nails had the fungal viability reduced. It is important to highlight that there are few works about the antibiofilm activity of surfactin, iturin, and fengycin against *Fusarium* biofilms. This important antifungal effect of lipopeptides from CE may have an impact, preventing the establishment of infection, fungal invasion, reinfection, and dissemination (da Silva et al. 2021).

Due to the better antifungal activity of CE on *F. solani*, it was also tested to determine its toxicity and antifungal efficacy using fibroblasts and the larval model of *G. mellonella*. CE at 100 µg/mL was not cytotoxic for human fibroblasts, and a dose of 100 mg/kg did not cause death or any health status reduction of the larvae. Falqueto and co-workers (Falqueto et al. 2021) reported that extracts containing lipopeptides obtained from *Bacillus velezensis* (strain B15) were not toxic for *G. mellonella*, *Caenorhabditis elegans*, *Scenedesmus obliquus*, and *Tetrahymena pyriformis* even as on murine fibroblasts (Da Silva et al. 2021), and other cell lineages (RAW 264.7 and VERO) (Falqueto et al. 2021).

Few works have shown biological effects of surfactins, iturins, and/or fengycins using animal models (Yan et al. 2017; Piewngam et al. 2018; Lei et al. 2019; Tsai et al. 2022; Chen et al. 2023), while in vivo studies of their antifungal effects on *Fusarium* spp. using plants or part of plants (e.g., seeds) are more frequent in the literature (Mihalache et al. 2018). In this regard, we used *G. mellonella* larvae as a proof of concept of systemic antifungal activity, and although CE treatment of *G. mellonella* infected with *F. solani* did not reduce the mortality rate, it reduced the fungal burden in the larval tissue, showing the inhibitory effect of lipopeptides on *F. solani* using an animal model. Together, our results and data from the literature support the idea of applying lipopeptides in the prevention and control of fungi, mainly *Fusarium* spp., promoting health care for humans and other animals.

In conclusion, twenty lipopeptides from the culture supernatant of an isolate of the *Bacillus subtilis* complex (strain UL-1) were characterized as the families iturins, fengycins, and surfactins and the high content was associated with higher hemolytic and antifungal effects. In addition, the mixture of lipopeptides in the crude extract demonstrated potent anti-adhesion and antibiofilm effects, supporting further studies for the use of these lipopeptides in the treatment and prevention of fusariosis.

Supplementary Information The online version contains supplementary material available at https://doi.org/10.1007/s00253-023-12712-z.

Acknowledgements The authors would like to thank Prof. Dr. Leticia Lotufo for kindly sharing the framework for cytotoxicity studies and Dr. Tatiana Reis and Marcela Gonçalves for their technical support in the laboratory.

Author contribution D. S. L. and C. C. S. performed the experiments, analyzed the results, and draft the manuscript. V. M. B. identified the bacterial isolate by molecular tools. J. C. S. C. and M. J. P. F. quantified the total lipopeptides by HPLC–DAD-UV. L. C. A. was responsible for the experimental design and data analysis of the cytotoxicity assays. F. S. C. A. contributed to obtaining the bacterial isolate. K. I. and M. S. designed the experiments, analyzed the data, and wrote and edited the manuscript. All authors have read and approved the manuscript before publication.

Funding This study was supported by the Fundação de Amparo à Pesquisa do Estado de São Paulo (FAPESP, 2021/01279–5 and 2020/16554–9), Conselho Nacional de Desenvolvimento Científico e Tecnológico (CNPq, 405556/2018–7), and Coordenação de Aperfeiçoamento de Pessoal de Nível Superior (CAPES). D. S. L. was a CAPES fellow (finance code 001), C. C. S. and J. C. S. C. were CNPq fellows (150534/2022–1 and 140120/2018–1, respectively), and V. M. B. was a FAPESP fellow (2018/11612–0). K. I. and M. J. P. F. are research fellows of the CNPq (306041/2022–7 and 308952/2020–0, respectively).

Data availability All data will be made available from the corresponding author upon request.

Declarations

Ethical approval This article does not contain any studies with human participants or animals performed by any of the authors.

Conflict of interest The authors declare no competing interests.

References

Adékambi T, Drancourt M, Raoult D (2009) The rpoB gene as a tool for clinical microbiologists. Trends Microbiol 17:37–45

Al-Hatmi AMS, Bonifaz A, Ranque S, Sybren de Hoog G, Verweij PE, Meis JF (2018) Current antifungal treatment of fusariosis. Int J Antimicrob Agents 51:326–332. https://doi.org/10.1016/j.ijantimicag.2017.06.017

Alonso-Monge R, Navarro-García F, Román E, Negredo AI, Eisman B, Nombela C, Pla J (2003) The Hog1 mitogen-activated protein kinase is essential in the oxidative stress response and chlamydospore formation in *Candida albicans*. Eukaryot Cell 2:351–361. https://doi.org/10.1128/EC.2.2.351-361.2003

Aranda FJ, Teruel JA, Ortiz A (2005) Further aspects on the hemolytic activity of the antibiotic lipopeptide iturin A. Biochim Biophys Acta - Biomembr 1713:51–56. https://doi.org/10.1016/j.bbamem.2005.05.003

Ben Ayed H, Nasri R, Jemil N, Ben Amor I, Gargouri J, Hmidet N, Nasri M (2015) Acute and sub-chronic oral toxicity profiles of lipopeptides from *Bacillus mojavensis* A21 and evaluation of their in vitro anticoagulant activity. Chem Biol Interact 236:1–6. https://doi.org/10.1016/j.cbi.2015.04.018

Bonmatin J-M, Laprévote O, Peypoux F (2003) Diversity among microbial cyclic lipopeptides: iturins and surfactins. Activity-structure relationships to design new bioactive agents. Comb Chem High Throughput Screen 6:541–556. https://doi.org/10.2174/138620703106298716

Bush K (2012) Antimicrobial agents targeting bacterial cell walls and cell membranes. OIE Rev Sci Tech 31:43–56. https://doi.org/10.20506/rst.31.1.2096

Cao Y, Pi H, Chandrangsu P, Li Y, Wang Y, Zhou H, Xiong H, Helmann JD, Cai Y (2018) Antagonism of two plant-growth promoting *Bacillus velezensis* isolates against *Ralstonia solanacearum* and *Fusarium oxysporum*. Sci Rep 8:1–14. https://doi.org/10.1038/s41598-018-22782-z

Ceresa C, Rinaldi M, Tessarolo F, Maniglio D, Fedeli E, Tambone E, Caciagli P, Banat IM, Diaz De Rienzo MA, Fracchia L (2021) Inhibitory effects of lipopeptides and glycolipids on *C. albicans–Staphylococcus* spp. dual-ppecies biofilms. Front Microbiol 11:1–19. https://doi.org/10.3389/fmicb.2020.545654

Chen X, Zhao H, Lu Y, Meng F, Lu Z, Lu Y (2023) Surfactin mitigates dextran sodium sulfate-induced colitis and behavioral disorders in mice by mediating gut-brain-axis Balance. J Agric Food Chem 71:1577–1592. https://doi.org/10.1021/acs.jafc.2c07369

Clinical and Laboratory Standards Institute (2017a) Document M27-A4. Ref Method broth dilution antifung suscetibility test yeasts. Approv Stand 4th ed

Clinical and Laboratory Standards Institute (2017b) Reference method for broth dilution M38. Ref Method Broth Dilution Antifung Susceptibility Test Filamentous Fungi Approv Stand 3th ed 28:0–13

Cochrane SA, Vederas JC (2016) Lipopeptides from *Bacillus* and *Paenibacillus* spp.: a gold mine of antibiotic candidates. Med Res Rev 36:4–31. https://doi.org/10.1002/med.21321

da Silva GO, Farias BCS, Da Silva RB, Teixeira EH, Cordeiro RDA, Hissa DC, Melo VMMI (2021) Effects of lipopeptide biosurfactants on clinical strains of *Malassezia furfur* growth and biofilm formation. Med Mycol 59:1191–1201. https://doi.org/10.1093/mmy/myab051

Falcão LL, Silva-Werneck JO, Vilarinho BR, da Silva JP, Pomella AWV, Marcellino LH (2014) Antimicrobial and plant growth-promoting properties of the cacao endophyte *Bacillus subtilis* ALB629. J Appl Microbiol 116:1584–1592. https://doi.org/10.1111/jam.12485

Falqueto SA, Pitaluga BF, de Sousa JR, Targanski SK, Campos MG, de Oliveira Mendes TA, da Silva GF, Silva DHS, Soares MA (2021) *Bacillus* spp. metabolites are effective in eradicating *Aedes aegypti* (Diptera: Culicidae) larvae with low toxicity to non-target species. J Invertebr Pathol 179:107525. https://doi.org/10.1016/j.jip.2020.107525

Gong AD, Li HP, Yuan QS, Song XS, Yao W, He WJ, Zhang JB, Liao YC (2015) Antagonistic mechanism of iturin a and plipastatin a from Bacillus amyloliquefaciens S76–3 from wheat spikes against Fusarium graminearum. PLoS One 10:e0116871. https://doi.org/10.1371/journal.pone.0116871

Gu Q, Yang Y, Yuan Q, Shi G, Wu L, Lou Z, Huo R, Wu H, Borriss R, Gao X (2017) Bacillomycin D produced by *Bacillus amyloliquefaciens* is involved in the antagonistic interaction with the plant pathogenic fungus *Fusarium graminearum*. Appl Environ Microbiol 83:e01075-17. https://doi.org/10.1128/AEM.01075-17

Hofemeister J, Conrad B, Adler B, Hofemeister B, Feesche J, Kucheryava N, Steinborn G, Franke P, Grammel N, Zwintscher A, Leenders F, Hitzeroth G, Vater J (2004) Genetic analysis of the biosynthesis of non-ribosomal peptide- and polyketide-like antibiotics, iron uptake and biofilm formation by *Bacillus subtilis* A1/3. Mol Genet Genomics 272:363–378. https://doi.org/10.1007/s00438-004-1056-y

Hou YH, Hsu LH, Wang HF, Lai YH, Chen YL (2020) Calcineurin regulates conidiation, chlamydospore formation and virulence in *Fusarium oxysporum* f. sp. lycopersici. Front Microbiol 11:2629. https://doi.org/10.3389/fmicb.2020.539702

Hue N, Serani L, Laprévote O (2001) Structural investigation of cyclic peptidolipids from *Bacillus subtilis* by high-energy tandem mass spectrometry. Rapid Commun Mass Spectrom 15(3):203–209. https://doi.org/10.1002/1097-0231(20010215)15:3%3c203::AID-RCM212%3e3.0.CO;2-6

Kim PI, Ryu J, Kim YH, Chi YT (2010) Production of biosurfactant lipopeptides iturin A, fengycin, and surfactin A from *Bacillus*

subtilis CMB32 for control of *Colletotrichum gloeosporioides*. J Microbiol Biotechnol 20:138–145. https://doi.org/10.4014/jmb.0905.05007

Jacques P (2011) Surfactin and other lipopeptides from *Bacillus* spp. In: Soberón-Chávez G (ed) Biosurfactants. Microbiology monographs, vol 20. Springer, Berlin. https://doi.org/10.1007/978-3-642-14490-5_3

Jemil N, Manresa A, Rabanal F, Ben Ayed H, Hmidet N, Nasri M (2017) Structural characterization and identification of cyclic lipopeptides produced by *Bacillus methylotrophicus* DCS1 strain. J Chromatogr B Anal Technol Biomed Life Sci 1060:374–386. https://doi.org/10.1016/j.jchromb.2017.06.013

Kato A, Hirata H, Ohashi Y, Fuji K, Harada K-I (2011) A new anti-MRSA antibiotic complex, WAP-8294A II. Structure characterization of minor components by ESI LCMS and MS/MS. J Antibiot 64:373–379. https://doi.org/10.1038/ja.2011.9

Kurtz MB, Heath IB, Marrinan J, Dreikorn S, Onishi J, Douglas C (1994) Morphological effects of lipopeptides against *Aspergillus fumigatus* correlate with activities against (1,3)-β-D-glucan synthase. Antimicrob Agents Chemother 38:1480–1489. https://doi.org/10.1128/AAC.38.7.1480

Lei S, Zhao H, Pang B, Qu R, Lian Z, Jiang C, Shao D, Huang Q, Jin M, Shi J (2019) Capability of iturin from *Bacillus subtilis* to inhibit *Candida albicans* in vitro and in vivo. Appl Microbiol Biotechnol 103:4377–4392. https://doi.org/10.1007/s00253-019-09805-z

Li L, Ma M, Huang R, Qu Q, Li G, Zhou J, Zhang K, Lu K, Niu X, Luo J (2012) Induction of chlamydospore formation in *Fusarium* by cyclic lipopeptide antibiotics from *Bacillus subtilis* C2. J Chem Ecol 38:966–974. https://doi.org/10.1007/s10886-012-0171-1

Liu Y, Lu J, Sun J, Zhu X, Zhou L, Lu Z, Lu Y (2019) C16-fengycin A affect the growth of *Candida albicans* by destroying its cell wall and accumulating reactive oxygen species. Appl Microbiol Biotechnol 103:8963–8975. https://doi.org/10.1007/s00253-019-10117-5

Loh JMS, Adenwalla N, Wiles S, Proft T (2013) *Galleria mellonella* larvae as an infection model for group A Streptococcus. Virulence 4:419–428. https://doi.org/10.4161/viru.24930

Lohse MB, Gulati M, Johnson AD, Nobile CJ (2018) Development and regulation of single-and multi-species *Candida albicans* biofilms. Nat Rev Microbiol 16:19–31

Luiz RLF, Vila TVM, de Mello JCP, Nakamura CV, Rozental S, Ishida K (2015) Proanthocyanidins polymeric tannin from *Stryphnodendron adstringens* are active against *Candida albicans* biofilms. BMC Complement Altern Med 15:68. https://doi.org/10.1186/s12906-015-0597-4

Ma LJ, Geiser DM, Proctor RH, Rooney AP, O'Donnell K, Trail F, Gardiner DM, Manners JM, Kazan K (2013) *Fusarium* pathogenomics. Annu Rev Microbiol 67:399–416. https://doi.org/10.1146/annurev-micro-092412-155650

Ma Y, Kong Q, Qin C, Chen Y, Chen Y, Lv R, Zhou G (2016) Identification of lipopeptides in *Bacillus megaterium* by two-step ultrafiltration and LC-ESI-MS/MS. AMB Express 6(1):79. https://doi.org/10.1186/s13568-016-0252-6

Maksimov IV, Singh BP, Cherepanova EA, Burkhanova GF, Khairullin RM (2020) Prospects and applications of lipopeptide-producing bacteria for plant protection (review). Appl Biochem Microbiol 56:15–28. https://doi.org/10.1134/S0003683820010135

Mihalache G, Balaes T, Gostin I, Stefan M, Coutte F, Krier F (2018) Lipopeptides produced by *Bacillus subtilis* as new biocontrol products against fusariosis in ornamental plants. Environ Sci Pollut Res 25:29784–29793. https://doi.org/10.1007/s11356-017-9162-7

Mnif I, Ghribi D (2015) Lipopeptides biosurfactants: mean classes and new insights for industrial, biomedical, and environmental applications. Biopolymers 104:129–147

Monnerat R, Praça LB, Silva EYY da, Montalvão S, Martins E, Soares CM, Queiroz PR (2018) Produção e controle de qualidade de produtos biológicos à base de Bacillus thuringiensis para uso na agricultura

Mosmann T (1983) Rapid colorimetric assay for cellular growth and survival: application to proliferation and cytotoxicity assays. J Immunol Methods 65:55–63. https://doi.org/10.1016/0022-1759(83)90303-4

Nishiyama Y, Uchida K, Yamaguchi H (2002) Morphological changes of *Candida albicans* induced by micafungin (FK463), a water-soluble echinocandin-like lipopeptide. J Electron Microsc (Tokyo) 51:247–255. https://doi.org/10.1093/jmicro/51.4.247

Nucci M, Anaissie E (2007) *Fusarium* infections in immunocompromised patients. Clin Microbiol Rev 20:695–704. https://doi.org/10.1128/CMR.00014-07

Ongena M, Jacques P (2008) *Bacillus* lipopeptides: versatile weapons for plant disease biocontrol. Trends Microbiol 16:115–125

Pan R, Bai X, Chen J, Zhang H, Wang H (2019) Exploring structural diversity of microbe secondary metabolites using OSMAC strategy: a literature review. Front Microbiol 10:1–20. https://doi.org/10.3389/fmicb.2019.00294

Papayannopoulos IA (1995) The interpretation of collision-induced dissociation tandem mass spectra of peptides. Mass Spectrom Rev 14:49–73. https://doi.org/10.1002/mas.1280140104

Park JS, Ryu GR, Kang BR (2022) Target mechanism of iturinic lipopeptide on differential expression patterns of defense-related genes against *Colletotrichum acutatum* in pepper. Plants 11:1267. https://doi.org/10.3390/plants11091267

Piewngam P, Zheng Y, Nguyen TH, Dickey SW, Joo HS, Villaruz AE, Glose KA, Fisher EL, Hunt RL, Li B, Chiou J, Pharkjaksu S, Khongthong S, Cheung GYC, Kiratisin P, Otto M (2018) Pathogen elimination by probiotic *Bacillus* via signalling interference. Nature 562:532–537. https://doi.org/10.1038/s41586-018-0616-y

Pueyo MT, Bloch C Jr, Carmona-Ribeiro AM, di Mascio P (2009) Lipopeptides produced by a soil *Bacillus megaterium* strain. Microb Ecol 57:367–378. https://doi.org/10.1007/s00248-008-9464-x

Seydlová G, Svobodová J (2008) Review of surfactin chemical properties and the potential biomedical applications. Cent Eur J Med 3:123–133

Spadari CC, De Bastiani FWMS, Lopes LB, Ishida K (2019) Alginate nanoparticles as non-toxic delivery system for miltefosine in the treatment of candidiasis and cryptococcosis. Int J Nanomedicine 14:5187–5199. https://doi.org/10.2147/IJN.S205350

Stein T (2005) *Bacillus subtilis* antibiotics: structures, syntheses and specific functions. Mol Microbiol 56:845–857

Steinke K, Mohite OS, Weber T, Kovács ÁT (2021) Phylogenetic distribution of secondary metabolites in the *Bacillus subtilis* species complex. mSystems 6:e00057-21. https://doi.org/10.1128/mSystems.00057-21

Sumi CD, Yang BW, Yeo IC, Hahm YT (2015) Antimicrobial peptides of the genus *Bacillus*: a new era for antibiotics. Can J Microbiol 61:93–103. https://doi.org/10.1139/cjm-2014-0613

Tsai WC, Wong WT, Hsu HT, Cheng YH, Yu YH, Chen WJ, Ho CL, Hsu HC, Hua KF (2022) Surfactin containing *Bacillus licheniformis*-fermented products alleviate dextran sulfate sodium-induced colitis by inhibiting colonic inflammation and the NLRP3 inflammasome in mice. Animals 12:3456. https://doi.org/10.3390/ani12243456

Van Dijck P, Sjollema J, Cammue BPA, Lagrou K, Berman J, d'Enfert C, Andes DR, Arendrup MC, Brakhage AA, Calderone R, Cantón E, Coenye T, Cos P, Cowen LE, Edgerton M, Espinel-Ingroff A, Filler SG, Ghannoum M, Gow NAR, Haas H, Jabra-Rizk MA, Johnson EM, Lockhart SR, Lopez-Ribot JL, Maertens J, Munro CA, Nett JE, Nobile CJ, Pfaller MA, Ramage G, Sanglard D, Sanguinetti M, Spriet I, Verweij PE, Warris A, Wauters J, Yeaman MR, Zaat SAJ, Thevissen K (2018) Methodologies for in vitro

and in vivo evaluation of efficacy of antifungal and antibiofilm agents and surface coatings against fungal biofilms. Microb Cell 5:300–326. https://doi.org/10.15698/mic2018.07.638

Velho RV, Medina LFC, Segalin J, Brandelli A (2011) Production of lipopeptides among *Bacillus* strains showing growth inhibition of phytopathogenic fungi. Folia Microbiol (Praha) 56:297–303. https://doi.org/10.1007/s12223-011-0056-7

Yan L, Wenfeng Z, Xiaoling W, Jianping G (2017) Foxo3a-dependent Bim transcription protects mice from a high fat diet via inhibition of activation of the NLRP3 inflammasome by facilitating autophagy flux in Kupffer cells. Oncotarget 8:34258–34267. https://doi.org/10.18632/oncotarget.15946

Yang H, Li X, Li X, Yu H, Shen Z (2015) Identification of lipopeptide isoforms by MALDI-TOF-MS/MS based on the simultaneous purification of iturin, fengycin, and surfactin by RP-HPLC. Anal Bioanal Chem 407:2529–2542. https://doi.org/10.1007/s00216-015-8486-8

Zhao H, Shao D, Jiang C, Shi J, Li Q, Huang Q, Rajoka MSR, Yang H, Jin M (2017) Biological activity of lipopeptides from *Bacillus*. Appl Microbiol Biotechnol 101:5951–5960. https://doi.org/10.1007/s00253-017-8396-0

Zhao H, Li J, Zhang Y, Lei S, Zhao X, Shao D, Jiang C, Shi J, Sun H (2018) Potential of iturins as functional agents: safe, probiotic, and cytotoxic to cancer cells. Food Funct 9:5580–5587. https://doi.org/10.1039/c8fo01523f

Zhao B, He D, Wang L (2021) Advances in *Fusarium* drug resistance research. J Glob Antimicrob Resist 24:215–219. https://doi.org/10.1016/j.jgar.2020.12.016